Materials and Structures (2022) 55:195
https://doi.org/10.1617/s11527-022-02020-9

ORIGINAL ARTICLE

Effect of fiber hybridization on mechanical properties of concrete

Fengzhen He · Luigi Biolzi · Valter Carvelli

Received: 28 January 2022 / Accepted: 4 August 2022 / Published online: 30 August 2022

Abstract Ten concrete mixtures, using long and medium length hooked-end and short wave-shaped steel fibers, were designed to experimentally investigate the effect of hybrid reinforcement on workability, drying shrinkage, and mechanical properties of hybrid steel fiber reinforced concrete. The steel fibers reduced the workability and drying shrinkage. Hybrid fibers, including long hooked-end steel fiber, can produce a synergistic effect on compressive strength. For the adopted materials, a linear relationship was observed between shrinkage strain and compressive strength. The tensile splitting strength increased with the volume fraction of the hybrid fibers. The hybrid steel fibers generated a synergistic effect on the tensile splitting strength, with an almost constant ratio of tension splitting strength to compressive strength of hooked-end steel fiber reinforced concrete. The use of long hooked-end steel fiber reinforcement led to a higher modulus of rupture, residual strength, and toughness than other mono fibers. Flexural strength increased with the increasing volume fraction of hybrid fibers. Residual strength of hybrid steel fiber reinforced concrete varied with fiber hybridization. Overall, a concrete reinforced with a hybrid mix of all the considered steel fibers had the best performance among the considered ones.

Keywords Concrete · Hybrid fiber · Synergistic effect · Workability · Shrinkage · Mechanical properties

1 Introduction

Concrete is one of the most widely used building materials due to its cost and unique properties [1–3]. However, plain concrete is susceptible to cracking because of its brittle nature and has relatively low failure strain [4–6]. Many studies have been published to improve the mechanical performance of concrete (see, for instance, [6–11]). The results showed that adding randomly distributed fibers can effectively improve tensile strength, toughness, and impact resistance. The effectiveness of the improvement varies with fiber material, fiber geometry, distribution, orientation and content.

The fracture process of concrete is a multi-scale process, from the onset and propagation of micro cracks to macro cracks [8, 9, 12]. The presence of

Supplementary Information The online version contains supplementary material available at https://doi.org/10.1617/s11527-022-02020-9.

F. He (✉) · L. Biolzi · V. Carvelli
Department A.B.C, Politecnico di Milano, Piazza Leonardo da Vinci 32, 20133 Milan, Italy
e-mail: fengzhen.he@polimi.it

L. Biolzi
e-mail: luigi.biolzi@polimi.it

V. Carvelli
e-mail: valter.carvelli@polimi.it

micro steel fibers with a relatively small diameter and large aspect ratio have a better effect on restricting the onset, extension, and coalescence of the micro cracks during loading [13, 14]. But, micro steel fibers could have a weak adhesion to matrix, leading to pull out and propagation of macro cracks. Whereas, macro steel fibers with relatively large diameters and lengths have considerable bonding strength with the matrix. They can bridge and restrain the extension of macro cracks [15]. But, the mono fiber reinforcement of concrete can only produce effect on cracks in its own scale.

The hybrid steel fiber reinforcement including both micro and macro steel fiber may produce a synergistic effect on the improvement of the mechanical properties. The randomly distributed hybrid fibers in concrete can arrest the coalescence and propagation of the micro cracks and bridging the macro cracks [1, 16–18]. These effects depend on the content, shape, and material of fibers.

Studies on fiber reinforced concrete, especially hybrid fiber reinforced concrete, have provided valuable knowledge and techniques for a wide range of engineering applications [16, 17, 19]. However, more in-depth understandings and extensive investigations are still needed, mainly on the optimization of the concrete reinforcement and mechanical properties, which are of considerable importance for cost-effective and load-carrying concrete structures. The volume fraction of the hybrid fiber, detailed in the literature, varies from 0.1 to 4.5%. The higher volume fraction may lead to higher tensile strength of the hybrid fiber reinforced concrete, but it can also increase the cost and reduce workability [20, 21]. Therefore, the mix optimization is needed for a broader application of the hybrid fiber reinforced concrete. Moreover, the fibers in concrete influence the fracture process [22–24], leading to the change of the mechanical properties, especially the relationships between mechanical properties. However, the research on the relationships of the mechanical properties of hybrid fiber reinforced concrete is limited compared to plain concrete.

In this study, the effect of hybrid reinforcement on the physical and mechanical performance of concrete was investigated considering: workability of the fresh concrete, drying shrinkage, compressive strength, tension splitting strength, and flexural performance. The influence of the volume fraction and hybridization type on the engineering properties and fracture characteristics were determined.

2 Materials and methods

2.1 Materials

Portland Cement CEM II/A-LL42.5R, river gravel with the maximum nominal size of 16 mm, and crushed limestone with the maximum nominal size of 22 mm have been adopted. The fine aggregate was river sand having a maximum size of 4 mm. The physical properties and grading curves of aggregates are shown in Table 1 and Fig. 1. The additive Aeternum Proof [25] was used to keep workability above class S3 according to EN 206:2013 + A1:2016 [26]. The tap water was adopted with a temperature of 22 °C.

Three kinds of commercial steel fibers (see Fig. 2) with different geometric shapes have been used. The short steel fiber had a waved shape, while the long and medium fibers have hooked-end. The properties of the steel fibers used in this study are listed in Table 2.

2.2 Mix design and specimen casting

Ten concrete mixtures were designed, as shown in Table 3. The mix ID includes fiber type (S, M, L) and its volume fraction to present the fiber content in each concrete mixture. For example, mix L1.3S0.2 represents the 1.3% volume fraction of long hooked-end steel fibers and 0.2% of short wave-shaped fibers in this mixture. PC is plain concrete, which serves as reference material. S0.43, M1.5, and L1.5 contain

Table 1 Physical properties of the aggregates

	Coarse aggregate		Fine aggregate
	River gravel	Crushed limestone	River sand
Density (kg/m^3)	2630	2737	2640
Water absorption	1.16%	1.05%	1.83%

mono-type steel fiber. In M0.87S0.13, M1.3S0.2, and M1.73S0.27, the volume ratios between M and S are the same, but the total volume fractions are 1.0%, 1.5%, and 2.0%, respectively. L0.65M0.65S0.2, L1.3S0.2, and L0.75M0.75 include hybrid fiber reinforcements with the same total volume fraction.

The concrete was mixed according to the following process. First, the aggregates were mixed for 2 min with 1/3 water. Then, cement, additive, and 2/3 water were added and mixed for 3 min. After that, fibers were added by hand slowly while mixing to have a uniform distribution. Then the specimens were cast according to the standard EN 12390-2-2019 [27]. The specimens were kept in the molds for 24 h. Subsequently, they were demolded and cured in the chamber with a temperature of 20 ± 2 °C and relative humidity 90 ± 3% until the testing.

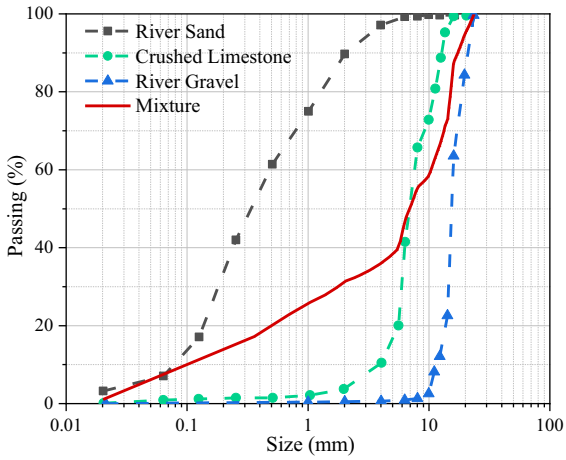

Fig. 1 Grading curves of the aggregates

2.3 Test methods

The compressive strengths after 1, 7, 28, and 56 days were measured on cubic specimens with a dimension of 100 mm according to the standard EN 12390-3:2019 [28]. Three specimens were tested for each mixture and each curing age. Tensile splitting tests were conducted on the cylindrical specimens with the dimensions of Diameter × Height = 150 mm × 300 mm at 28 days, according to the standard of EN 12390-6:2009 [29]. The flexural performance was investigated by three-point-bending testing on the notched prismatic specimens of Length × Width × Height = 600 mm × 150 mm × 150 mm according to the standard EN 14651:2005 + A1:2007 [30]. A notch with the dimensions of Depth × Wide = 25 mm × 5 mm was made on the mid-length specimen. The supports distance was 500 mm. The loading was controlled by the crack mouth opening displacement (CMOD). The speed of the CMOD was set at 0.05 mm/min before reaching 0.1 mm and then increased to 0.2 mm/min.

The shrinkage strain of the concrete mixtures during the first 56 curing days (after 1, 3, 7, 14, 28 and 56 days) was monitored according to the standard EN 12390–16:2019 [31]. The shrinkage of three prismatic specimens for each concrete mixture with the dimensions of Length × Width × Height = 500 mm × 100 mm × 100 mm was tested. The relative humidity of the chamber was (90 ± 3%). Therefore,

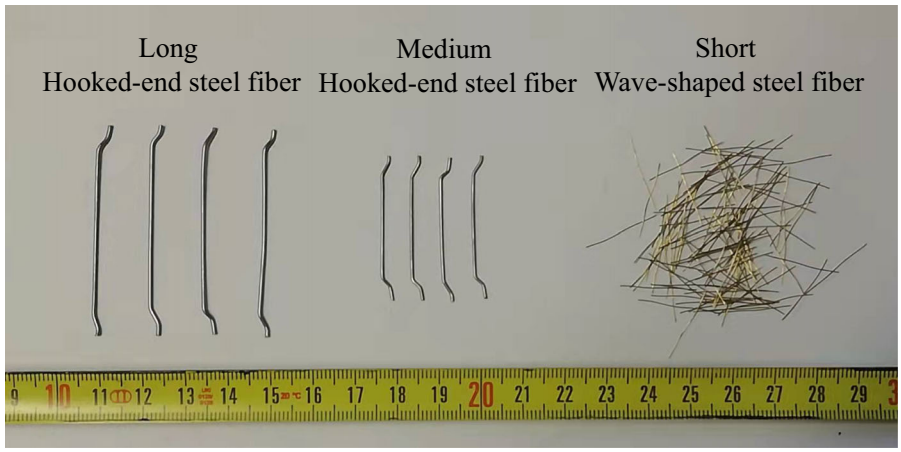

Fig. 2 Steel fibers used in this study

the shrinkage measured in this study was mainly related to the autogenous shrinkage. Moreover, the workability of fresh concrete was determined by conducting the slump test according to the standard EN 12350–2:2019 [32].

During the bending test, the digital image correlation (DIC) technique was adopted to monitor the development of the fracture process zone. The region of interest (ROI) was randomly speckled with black matte spray paint. The tests were assisted with a digital camera (Nikon D800), equipped with an adjustable lens with a focal length from 24 to 85 mm, located approximately 30 cm from the inspected surface. The camera acquired frames at a frequency of 1 Hz with a resolution of 5520 × 3680 pixels, with a scale factor of 5.78 μm/pixel.

Table 2 Properties of steel fibers

	Long (L) hooked-end	Medium (M) hooked-end	Short (S) wave-shaped
Length (mm)	50	35	18
Diameter (mm)	1.05	0.75	0.2
Aspect ratio (L/D)	48	47	90
Density (kg/m^3)	7800	7800	7800
Tensile Strength (N/mm^2)	1440	1250	2600
Modulus of elasticity (GPa)	200	200	200

3 Experimental results and analyses

3.1 Workability

The slump test was adopted for determining the consistency and workability of the fresh concrete. The slump testing results of concrete mixtures are shown in

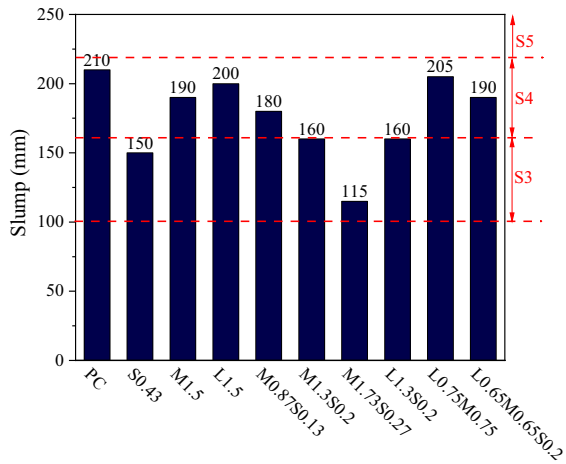

Fig. 3 Slump of concrete mixtures

Table 3 Concrete mixtures

Mix ID	W/C	Cement (kg/m^3)	Aggregate (kg/m^3)			Volume fraction of fiber (%)			Additive (kg/m^3)
			River gravel	Crushed limestone	River sand	Long	Medium	Short	
PC	0.45	450	735	562	361	–	–	–	13.5
S0.43★			730	550	345	–	–	0.43	
M1.5			705	530	320	–	1.5	–	
L1.5			705	530	320	1.5	–	–	
M0.87S0.13			725	550	320	–	0.87	0.13	
M1.3S0.2			705	530	320	–	1.3	0.2	
M1.73S0.27			705	530	320	–	1.73	0.27	
L0.65M0.65S0.2			705	530	320	0.65	0.65	0.2	
L1.3S0.2			705	530	320	1.3	–	0.2	
L0.75M0.75			705	530	320	0.75	0.75	–	

★ 0.43% is the maximum volume fraction of short fibers. Beyond this volume fraction, many fiber clumps appear in the concrete

Fig. 3. According to the standard EN 206:2013 + A1:2016 [26], the results can be collected into the five classes from S1 to S5. In real applications, the fresh concrete transported by the pump should have a slump belonging to S4 or S5. As can be seen from Fig. 3, adding steel fiber reduces the workability of the fresh concrete. The short wave-shaped steel fibers produce a more considerable reduction effect on workability than hooked-end steel fibers. For example, only 0.43% short wave-shaped fiber in S0.43 reduces the slump to 150 mm, which belongs to the S3 class, but 1.5% long (L1.5) and medium (M1.5) hooked-end steel fiber produce a smaller decrease compared to PC. It could be related to the larger aspect ratio of short wave-shaped steel fiber [2]. The increasing volume fraction of the hybrid fiber has a negative effect on the workability of fresh concrete. The slump decreases from 180 to 115 mm when the volume fraction increases from 1.0% (M0.87S0.13) to 2.0% (M1.73S0.27). The higher volume fraction increases the interaction between the steel fibers, reducing the fluidity of the fresh concrete [2, 33]. For concrete including hybrid fibers with the same volume fraction but different combinations, the slumps vary with hybridization type. Hybrid fibers containing short wave-shaped steel fibers had an evident reduction effect on the workability of fresh concrete. Except for S0.43 and M1.73S0.27, the workability of concrete mixtures belongs to S4.

3.2 Shrinkage

The shrinkage strain of concrete is mainly related to autogenous and drying one. The humidity of the chamber was 90 ± 3% during the whole testing period. Therefore, the drying shrinkage was negligible and the shrinkage, in this study, was mainly autogenous (hydration reaction [34, 35]).

The shrinkage strain measurements for different curing times up to 56 days are presented in Fig. 4. Figure 4a shows the shrinkage strain of concrete, including mono fibers. Mono steel fibers reinforced concrete clearly shows a reduction of the shrinkage strain. The short wave-shaped steel fibers had a better effect on reducing shrinkage strain than hooked-end steel fibers. The order of the shrinkage is PC > L1.5 > M1.5 > S0.43. It is mainly motivated by the larger aspect ratio of short wave-shaped steel fiber, which produces a better effect on arresting the micro-cracks caused by the shrinking tensile stress [36, 37]. Moreover, the medium hooked-end steel fibers were more effective than the long hooked-end steel fibers.

The influence of the volume fraction on shrinkage is indicated in Fig. 4b. The shrinkage of hybrids fiber reinforced concrete increased significantly when the volume fraction exceeded 1.0%. The shrinkage strain at 56 days grew from 197 × 10^{-6} (M0.87S0.13) to 246 × 10^{-6} (M1.73S0.27) when the volume fraction increased from 1.0% to 2.0%. But shrinkage strains were still lower than that of PC. Hybrid fibers produced the positive effect of reducing shrinkage by constraining the micro-crack propagation during the hardening process [38].

Figure 4c shows the shrinkage strains of concrete with different combinations of hybrid fibers. The considered fiber combinations have a negligible effect on shrinkage strain. The shrinkage strains of L1.3S0.2 and L0.65M0.65S0.2 at 56 days were similar to L1.5. But the shrinkage strains of L1.3S0.2 and L0.65M0.65S0.2, including short wave-shaped steel fiber, were lower than that of L0.75M0.75. It may be caused by the adverse effect of the long hooked-end steel fibers and the better bridging effect of short wave-shaped steel fibers.

3.3 Compressive strength

The compressive strength of concrete mixtures during the first 56 days is shown in Fig. 5. Mono fiber with different shapes produced similar effects on the compressive strength, as shown in Fig. 5a. The compressive strengths fluctuate close to that of PC. It could be connected to the voids and micro cracks created by steel fibers [2, 38], which from the one hand create local stress concentrations and, from the other, delay the cracks propagation (bridging effect), restricting macroscopically the lateral expansion, as well [39].

Figure 5b describes the influence of the volume fraction of the hybrid reinforcement on the development of compressive strength. After the same curing time, compressive strengths decreased when the volume fraction increased from 0% to 1.0% or 1.5%. With a volume fraction of 2%, compressive strength was at the same level as PC. The fluctuation of the compressive strength with the increasing volume fraction is attributed to the interaction of the

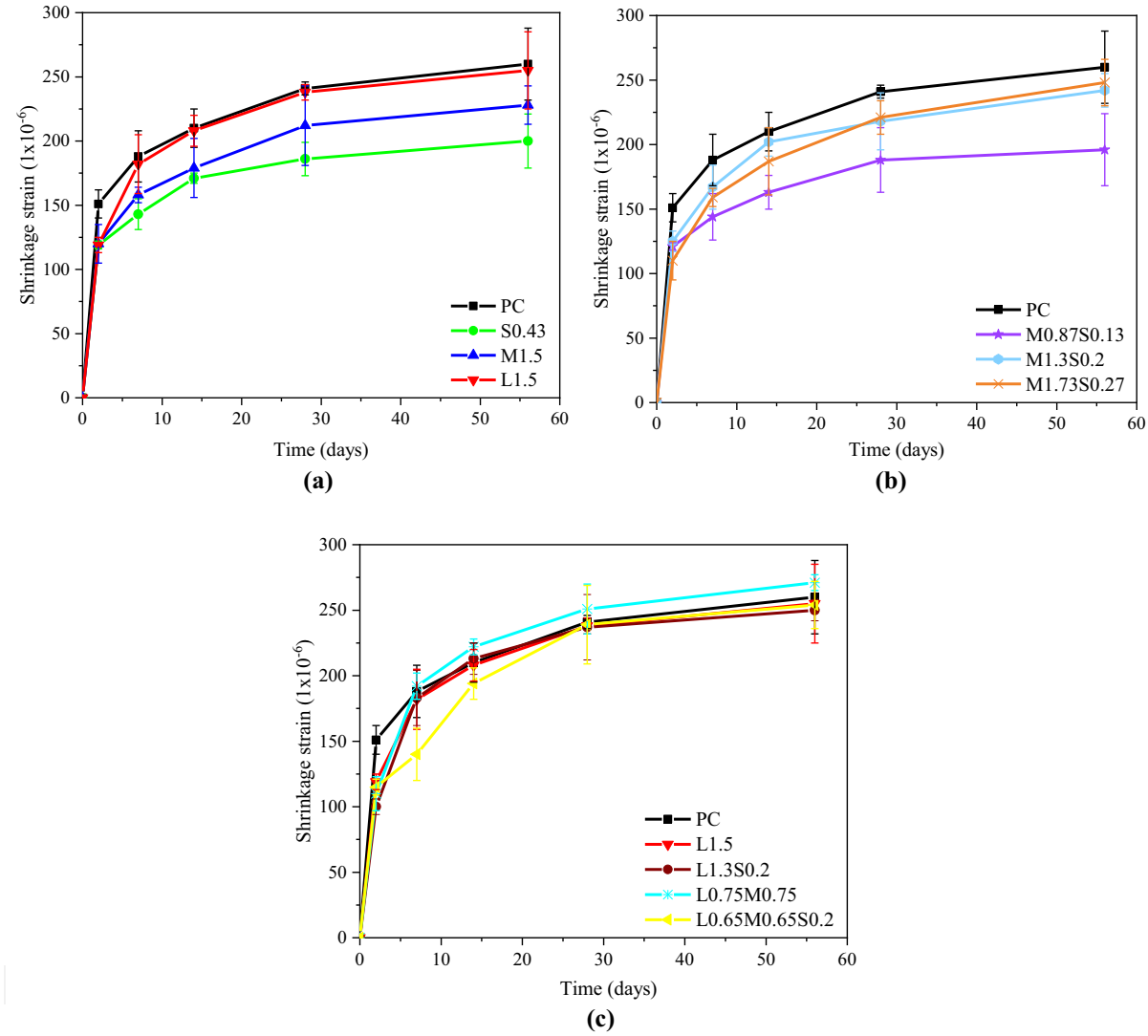

Fig. 4 Shrinkage strain of concrete mixture: **a** mono fiber, **b** hybrid fiber with different volume fractions, **c** different hybrid fiber combinations. Error bars show the standard deviation of 3 replicas

introduced pores and the confinement effect of hybrid fibers, enhanced by the higher content.

The influence of the combination of hybrid steel fiber on the compressive strength is shown in Fig. 5c. The hybrid fibers with different combinations produced a synergistic effect compared to mono steel fiber. Compressive strengths of L0.65M0.65S0.2, L0.75M0.75, and L1.3S0.2 at 56 days are 16.8%, 1.9% and 5.5% higher than that of L1.5. The possible reason is the hybrid fiber produces a much effective bridging effect at different crack scales. It is worth noting that L0.65M0.65S0.2 has a more substantial synergistic effect than L0.75M0.75 and L1.3S0.2. The mix L0.65M0.65S0.2, containing three kinds of steel fiber, can arrest the propagation of both micro and macro cracks more effectively [9, 17], leading to higher compressive strength.

As depicted in Fig. 6, an almost linear relationship was detected between shrinkage strain and compressive strength for all considered concrete mixtures. A similar linear relationship was reported in mortar [40] and plain concrete [41]. The coefficients of correlation can assess the reliability of the linear interpolation. Except for S0.43, the coefficients of correlation are

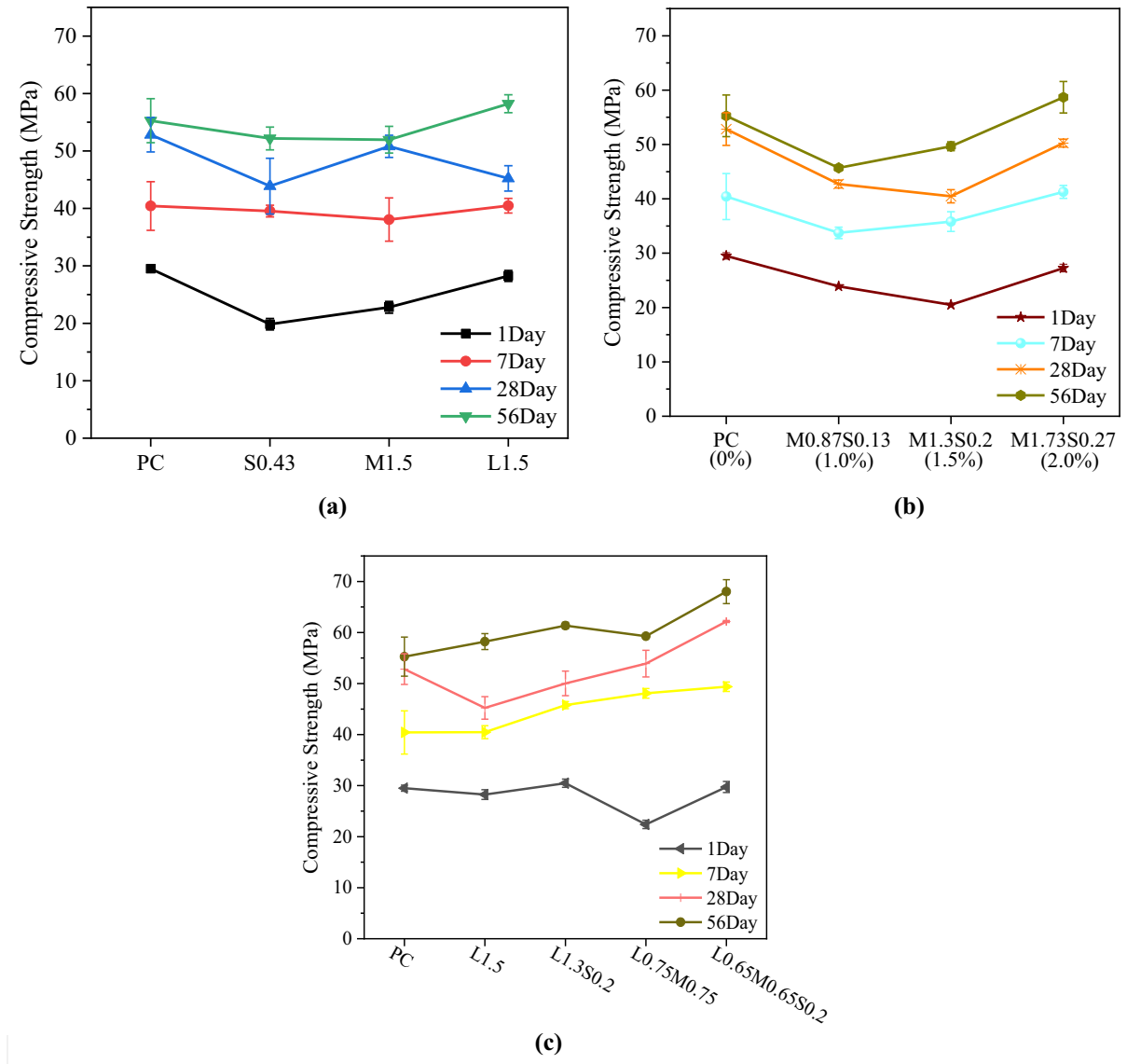

Fig. 5 Compressive strength of concrete mixture: **a** mono fiber, **b** hybrid fiber with different volume fractions, **c** other hybrid fiber combinations. Error bars show the standard deviation of 3 replicas

above 0.8. This liner relationship highlighted the proportional evolution in time of the autogenous shrinkage and the compressive strength and their correlation during the hydration process.

3.4 Tensile splitting strength

The tensile splitting strengths of the concrete mixtures at 28 days are shown in Fig. 7. The adding of the steel fibers, regardless of the combination type and volume fraction, improved the tensile splitting strength compared to PC. The tensile splitting strengths of fiber reinforced concrete ranged from 3.56 MPa to 6.16 MPa, which were higher than the 3.46 MPa of the plain concrete. The mono fiber reinforcement produced an increased ratio between 2.9% and 49.4% compared to PC (see Fig. 7a). The hybrid fibers with long hooked-end steel fiber improved the tensile splitting strength by 2.9%, 9.9%, and 19.1% compared to L1.5 (see Fig. 7c).

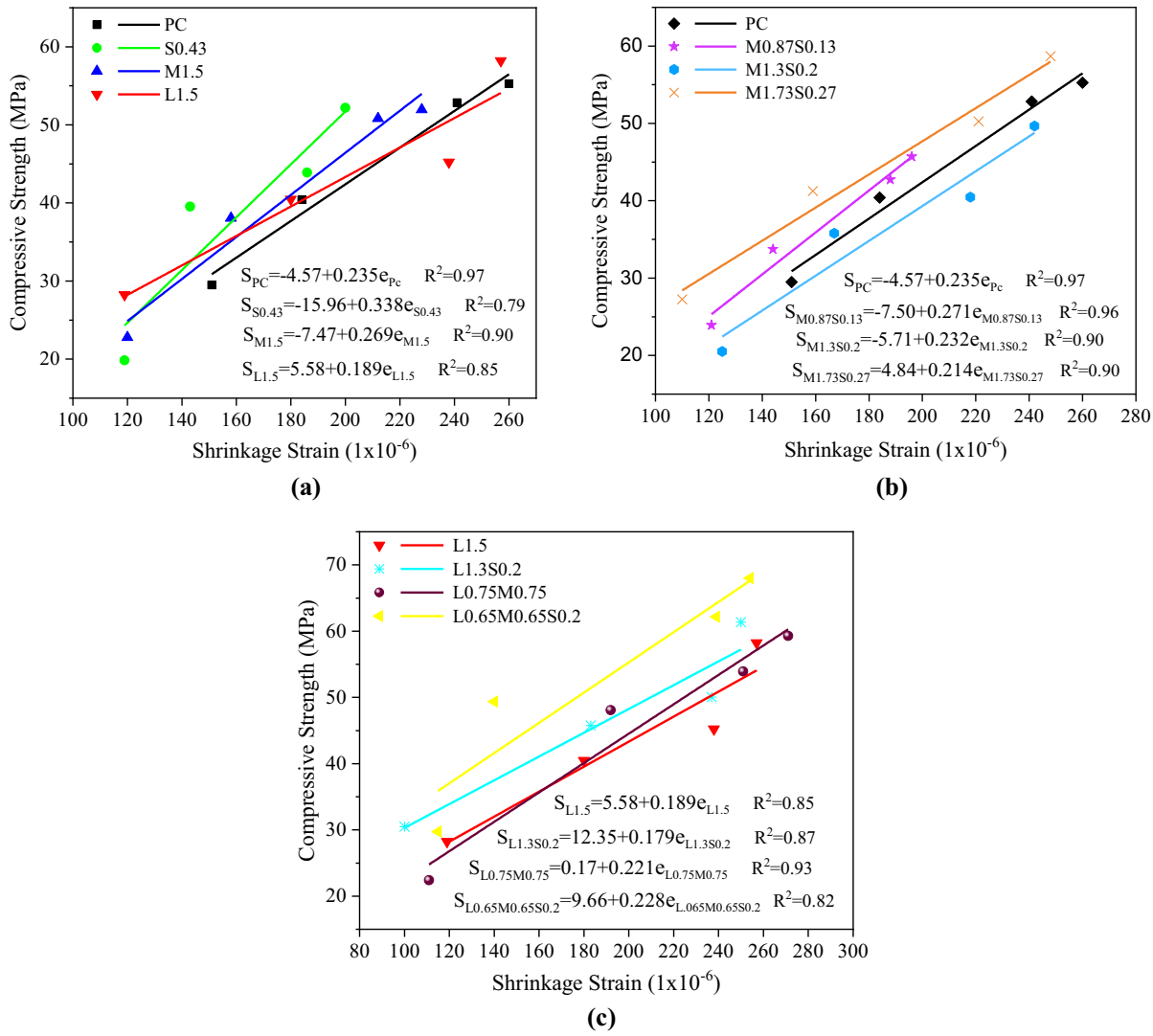

Fig. 6 Relationship between the compressive strength and the shrinkage strain: **a** mono fiber, **b** hybrid fiber with different volume fractions, **c** different hybrid fiber combinations

Figure 7a presents the influence of the mono fiber on the tensile splitting strength. S0.43 produces a similar tension splitting strength to PC. However, the tensile splitting strengths of M1.5 and L1.5 increase by 41.0% and 49.4% compared to PC, reaching 4.88 MPa and 5.17 MPa, respectively. It can be explained by the inhibitory effect of fibers on crack propagation. The short wave-shaped steel fiber prevents the formation and propagation of the micro cracks, delaying coalescence process of micro cracks [23]. But, they have a negligible effect on the propagation of the macro cracks as they are pulled out with the formation of macro cracks. The hooked-end steel fiber has higher pull-out strength. Therefore, the hooked-end steel fiber can bridge macro cracks and transfer stress between both sides of the macro cracks [18]. These beneficial effects arrest the propagation of the macro cracks and reduce the stress concentration at the crack tip, improving the tensile splitting strength. The failure modes provide evidence of the above analysis (see Supplementary Information, Figure S1). Only one macro crack is visible on the surface of PC and S0.43. While the macro cracks surrounded by many small cracks on the surface of L1.5 and M1.5 indicate the bridging effect of the hooked-end steel fiber. The long hooked-end steel fiber produced a higher improvement

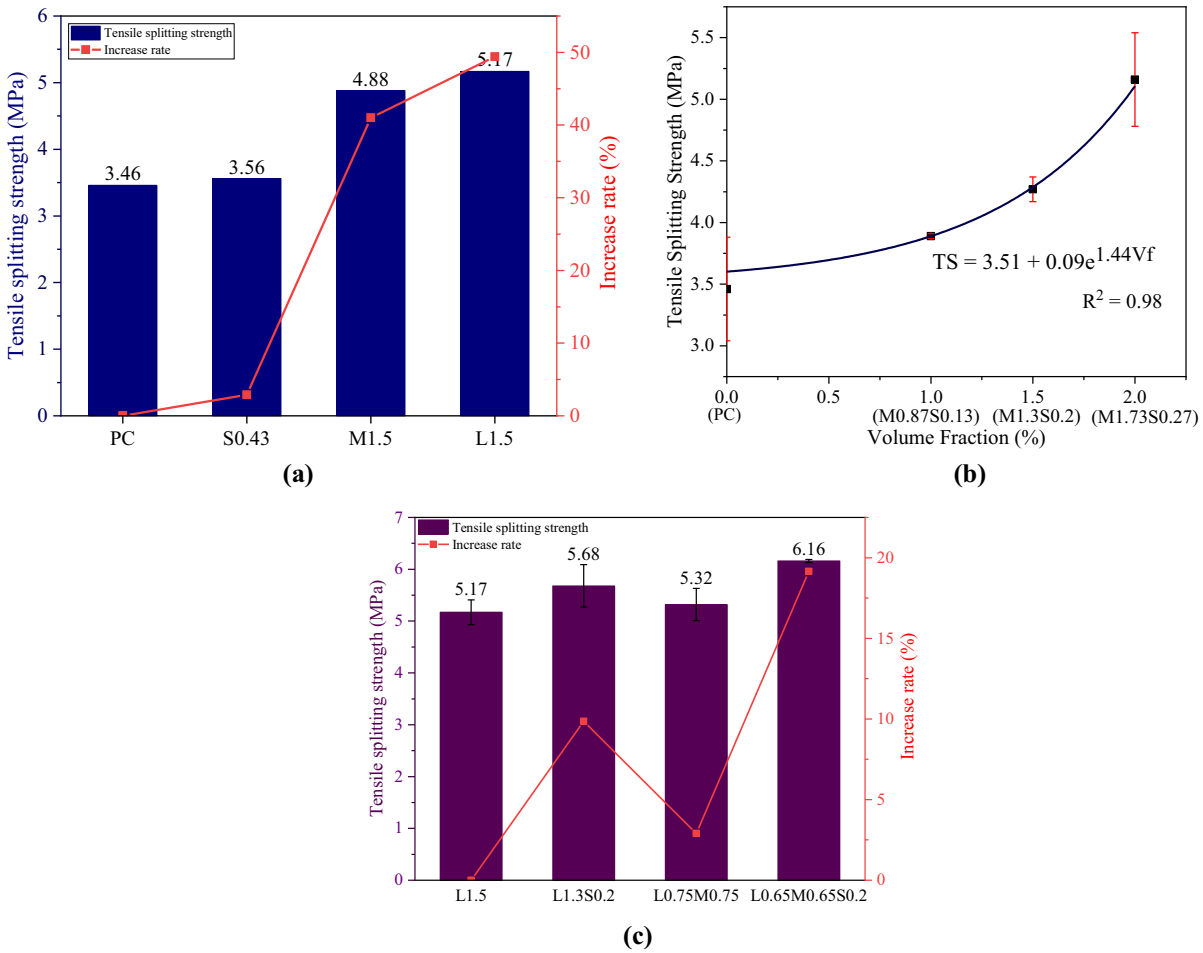

Fig. 7 Tensile splitting strength of concrete mixtures: **a** mono fiber, **b** hybrid fiber with different volume fractions, **c** different hybrid fiber combinations. Error bars show the standard deviation of 3 replicas

on the tensile splitting strength than the medium hooked-end steel fiber. It is attributed to the higher tensile strength and bonding strength of the long hooked-end steel fiber.

Figure 7b shows the tensile splitting strength of hybrid fiber reinforced concrete with different volume fractions. Tensile splitting strength increases from 3.46 MPa to 5.16 MPa when the volume fraction increases from 0% to 2.0%. It is possible to predict the tensile splitting strength as a function of the volume fraction of hybrid fiber by an exponential relationship:

$$TS = aTS_0 + be^{kV_f} \quad (1)$$

where TS is the tension splitting strength, TS_0 is the tensile strength of plain concrete, V_f is the volume fraction of the hybrid fiber (%), a, b and k are constants. In Fig. 7b, TS_0 is 3.46, while the best fitting provided a, b and k as 1.01, 0.09, and 1.44, respectively, with a coefficient of correlation of 0.98. Equation (1) is valid only in the considered volume fraction range ($\leq$ 2%) and the concrete mixes in this study; experimental measurements do not support further extrapolations.

The effect of the hybrid fibers with different combinations is presented in Fig. 7c. Hybrid fibers produce a synergistic effect on the tensile splitting strength. Tensile splitting strengths of L1.3S0.2, L0.75M0.75, and L0.65M0.65S0.2 are 5.68 MPa, 5.32 MPa, and 6.16 MPa, higher than the 5.17 MPa of L1.5. Hybrid fibers, including short wave-shaped fiber and hooked-end fiber, like L1.3S0.2 and L0.65M0.65S0.2, had a better beneficial effect than the hybrid hooked-end

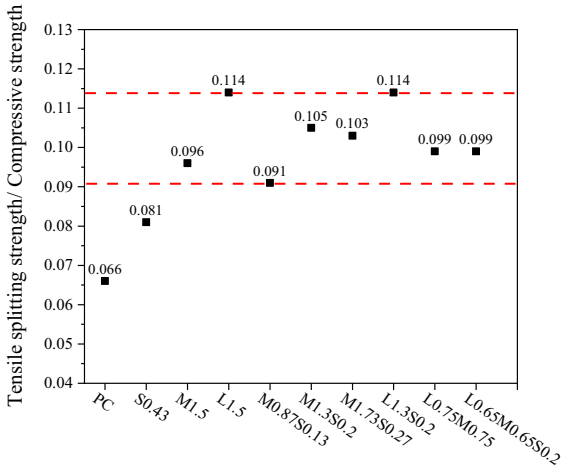

Fig. 8 Ratios between tensile splitting strength and compressive strength

fibers. Short wave-shaped fibers worked actively on restricting the propagation of the micro cracks, delaying the formation of macro cracks. Once the macro cracks appeared, short wave-shaped fibers were pulled out, and the hooked-end steel fibers bridged the macro cracks. The propagation of the macro cracks was restricted, and stress concentration was reduced. This is visible considering the multi-cracks failure modes of the hybrid fiber reinforced concrete (see Supplementary Information, Figure S1).

Figure 8 presents the relationships between the tensile splitting strength and compressive strength of concrete mixtures at 28 days. The ratio increases by adding steel fiber. For plain concrete, the ratio is 0.066. However, the ratio ranges from 0.091 to 0.114 for concrete mixtures, including hooked-end steel fibers. The range is similar to that obtained by Nataraja et al. [42] and Choi and Yuan [7]. Except for S0.43, the ratios are in a relatively narrow range between 0.091 and 0.114. Therefore, reasonable accuracy makes it possible to predict the tensile splitting strength of the steel fiber reinforced concrete containing hooked-end steel fibers according to the compressive strength, assuming the average ratio of 0.102.

3.5 Flexural performance

3.5.1 Flexural Stress-CMOD curve

Figure 9a depicts typical flexural stress-CMOD curves. Steel fibers improve flexural behavior and change the shape of the flexural stress-CMOD curve. The flexural stress of PC increased almost linearly up to the maximum flexural stress; then, it decreased sharply showing a brittle failure. For steel fiber reinforced concrete, a nonlinear behavior appeared before the peak load, exhibiting a pseudo strain hardening behavior with an increase of load after the level at the onset of initial crack. It is probably connected to the good bond of fibers and matrix, leading to a proper load transfer by the fibers at the early stage of the crack propagation.

After the peak point, the reinforced materials exhibited softening behavior, with loading levels slowly decreasing while increasing CMOD. This is a consequence of the fibers bridging effect resulting in a higher global bending deformation with relevant increasing of the post-peak residual flexural strength.

For mono-fiber reinforced concrete, long hooked-end steel fibers produced a higher improvement on flexural peak stress. For the hybrid steel fiber with the same combination (M and S), the higher volume fraction of the hybrid fiber leads to better flexural performance. The hybrid mixes with the same content (L0.75M0.75, L1.3S0.2, and L0.65M0.65S0.2) showed the best flexural response, both in terms of hardening and post peak behavior, quite similar to L1.5, which still highlighted the role of the long hooked-end fibers in constraining the development of meso/macro cracks.

Figure 9b summarizes the modulus of rupture (MOR) of concrete mixtures. Modulus of rupture is defined as the flexural strength at the peak load. The inclusion of steel fibers, regardless of the volume fraction and combination type, increases MOR. MOR of fiber reinforced concrete mixtures range from 4.59 to 10.81 MPa, increased by 15.3% to 171.6% compared with PC. It is mainly attributed to the bridging and arresting effect of the steel fiber [18, 43]. For the mono steel fiber, the MOR of L1.5 and M1.5 are higher than that of S0.43. It is due to the pull-out of short steel fibers at the appearance of macro cracks, while the hooked-end steel fiber still effectively transferred the stress across macro cracks [16, 23]. Therefore, concrete, including hooked-end steel fiber, can bear a higher flexural load.

MOR increases with the volume fraction of hybrid steel fiber. Figure 9b shows that the MOR increases from 5.39 to 7.64 MPa when the volume fraction increases from 1.0 to 2.0%. The increased number of

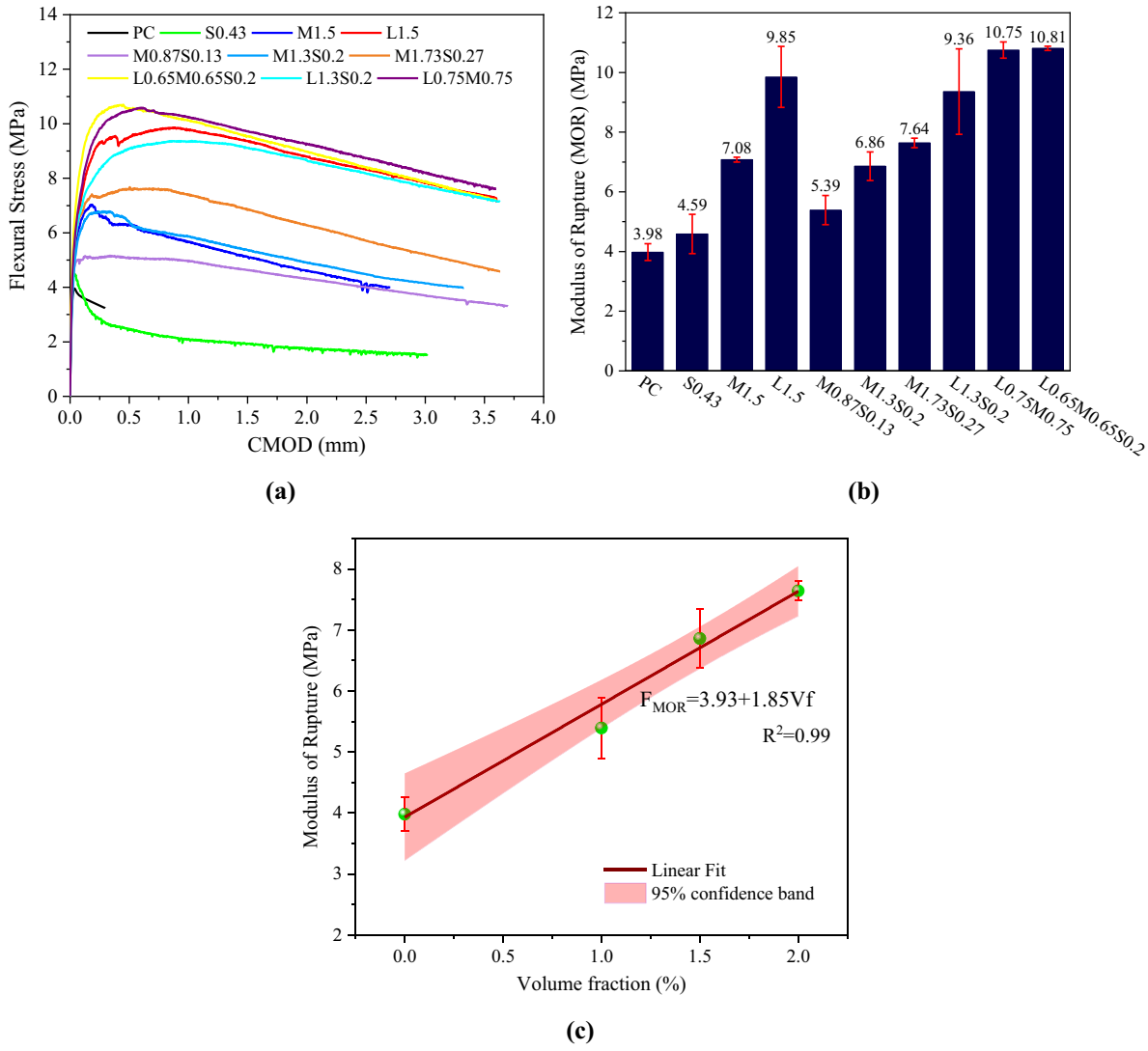

Fig. 9 Flexural properties: **a** flexural Stress-CMOD curves; **b** modulus of rupture; **c** relationship between volume fraction and modulus of rupture. The band and the error bars show the 95% confidence level and the standard deviation of 3 replicas, respectively

fibers enhanced the crack restriction effect, leading to a higher loading bearing capacity. According to Fig. 9c, there was a linear relation between MOR and volume fraction, as given by Eq. (2).

$$F_{MOR} = aF_{MOR,0} + kV_f \quad (2)$$

where F_{MOR} is the modulus of rupture, $F_{MOR,0}$ is the modulus of rupture of PC, a and k are constants, V_f is the volume fraction of hybrid fiber (%). According to the testing data, a is 1, and k is 1.85.

The considerable effect of the long hooked-end steel fiber is clearly detected by the highest MOR in the same experimental scatter band for all hybrid reinforcements, including L fibers (L1.5, L0.65M0.65S0.2, L1.3S0.2, and L0.75M0.75).

The ratios of MOR to compressive strength at 28 days are shown in Fig. 10. The steel fiber reinforcement increased the ratio compared to PC, from 0.075 (PC) to 0.218 (L1.5). The long hooked-end steel fiber produced a higher ratio than that of S0.43 and M1.5. It is attributed to the higher bonding strength between the long hooked-end steel fiber and cement matrix. The ratios of hybrid fiber reinforcement fluctuate with the increase of the volume fraction, which could be attributed to the variation of bonding strength, air voids, and micro cracks with the

increasing volume fraction. As mentioned above, the hybrid fibers combinations with long hooked-end steel fiber produce a synergistic effect, comparable to L1.5. The ratio of L0.65M0.65S0.2, L1.3S0.2 and L0.75M0.75 reached 0.174, 0.187 and 0.199, respectively.

3.5.2 *Residual flexural strength*

Residual flexural strength is an effective index for evaluating the contribution of the fibers on the post cracking performance of concrete. The residual flexural strength was investigated according to the standard of EN 14651:2005 + A1:2007. The limit of proportionality (LOP) is the stress at the tip of the notch, which is assumed to act in an uncracked mid-span section with linear stress distribution of the specimen subjected to the center-point load [30]. Conventionally, the LOP corresponds to the maximum force for CMOD lower than 0.05 mm, and the residual strength is estimated for CMOD of 0.5 mm, 1.5 mm, 2.5, and 3.5 mm. The corresponding flexural strengths are named f_{LOP}, $f_{R0.5}$, $f_{R1.5}$, $f_{R2.5}$, and $f_{R3.5}$. The comparison of the flexural strengths is shown in Fig. 11.

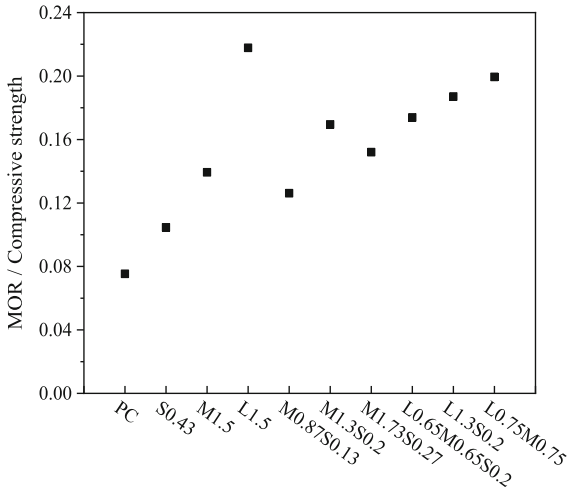

Fig. 10 Relationship between MOR and compressive strength

Figure 11a depicts the f_{LOP} of concrete mixtures. As it can be seen, the inclusion of steel fibers increases the f_{LOP}. Compared to PC, the average f_{LOP} of M1.5 and L1.5 were increased by 42.6% and 41.1%, while the S0.43, containing 0.43% short wave-shaped steel fiber, did not show enhancement having values in the same experimental scatter. It is a consequence of the higher bonding strength of hooked-end steel fibers, leading to a slower crack propagation. The higher volume fraction of the hybrid fiber produces the higher f_{LOP}. The average f_{LOP} increased from 4.94 MPa to 6.07 MPa when the volume fraction rose from 1.0% (M0.87S0.13) to 2.0% (M1.73S0.27). For concrete mixtures with different combination types of fiber, hybrid fibers produced the synergistic effect on f_{LOP}.

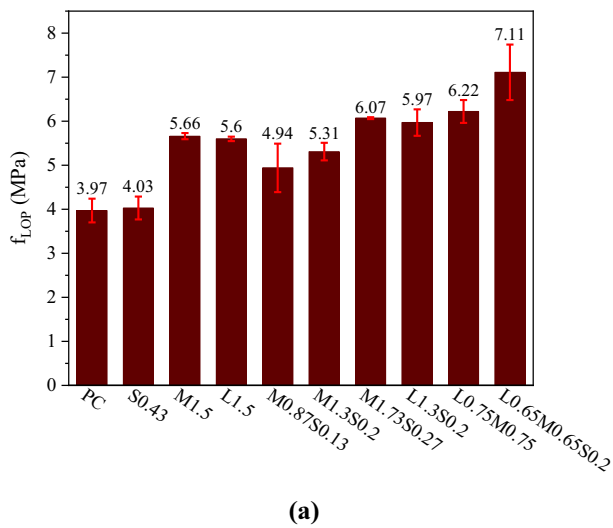

(a)

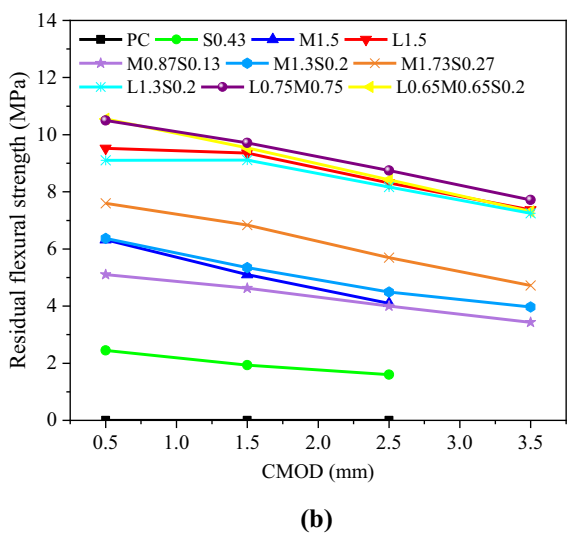

(b)

Fig. 11 Flexural strengths of concrete mixtures: **a** f_{LOP} and **b** average residual flexural strengths. Error bars show the standard deviation of 3 replicas

L0.65M0.65S0.2 has the highest f_{LOP} of 7.11 MPa, 27.0% and 25.6% higher than that of L1.5 and M1.5, respectively. Hybrid fiber, including steel fibers with different geometric parameters, can bridge and arrest both micro- and macro-crack. On the other hand, the hybrid fibers transfer stress more effectively in the concrete, reducing the stress concentration.

The residual flexural strengths of concrete mixtures are presented in Fig. 11b. The steel fiber reinforcement enhanced the residual flexural strengths. PC has no residual flexural strength as the specimen suddenly splits into two parts after the peak load, as shown in Fig. 9. L1.5 produced a more significant improvement on the residual flexural strength than M1.5 and S0.43. The short wave-shaped steel fibers were pulled with the extension of the macro cracks (see Supplementary Information, Figure S2). Therefore, the short wave-shaped fibers had a negligible effect on the propagation of the macro cracks. However, the hooked-end steel fibers can bridge the macro cracks with the higher bonding strength (see M1.5 and L1.5 in the Supplementary Information, Figure S2), slowing down the propagation of macro cracks and branching phenomena the crack path [18].

The residual flexural strength of the hybrid fiber reinforced concrete increases with the volume fraction. For example, the residual flexural strengths of M1.73S0.27 are from 37.6 to 49.0% higher than that of M0.87S0.13. Higher volume fraction provided higher bond strength in the unit flexural surface. Therefore, the extension of the macro cracks was arrested more effectively, evidenced by the branching cracking paths in M1.5 and L1.5 (see Supplementary Information, Figure S2). The hybrid fibers with the same volume fraction but different combination types produced a similar effect on the residual flexural strength compared to mono long hooked-end steel fiber (L1.5). Residual strengths of L0.75M0.75, L1.3S0.2, and L0.65M0.65S0.2 are similar to L1.5. It is because the hooked-end steel fibers played a major role in bridging and arresting the macro cracks after the peak load, as the short wave-shaped fibers were pulled out.

3.5.3 *Toughness and ductility*

Toughness indicates the energy-absorbing ability of concrete under loading, which can be obtained by integrating the area underneath the load–displacement curve (Fig. 12a). The toughness at the peak load (T_p) and 3.0 mm ($T_{3.0}$) deflection points were calculated. The results are summarized in Fig. 12b.

Steel fibers, especially the long hooked-end steel fibers, increase fracture toughness. For mono steel fibers, the long hooked-end steel fiber produced the highest T_p and $T_{3.0,}$ but the short wave-shaped fiber has a negligible effect on the T_p. The hooked-end steel fiber bridged the macro cracks, making the concrete bear a higher peak load. The toughness of fiber

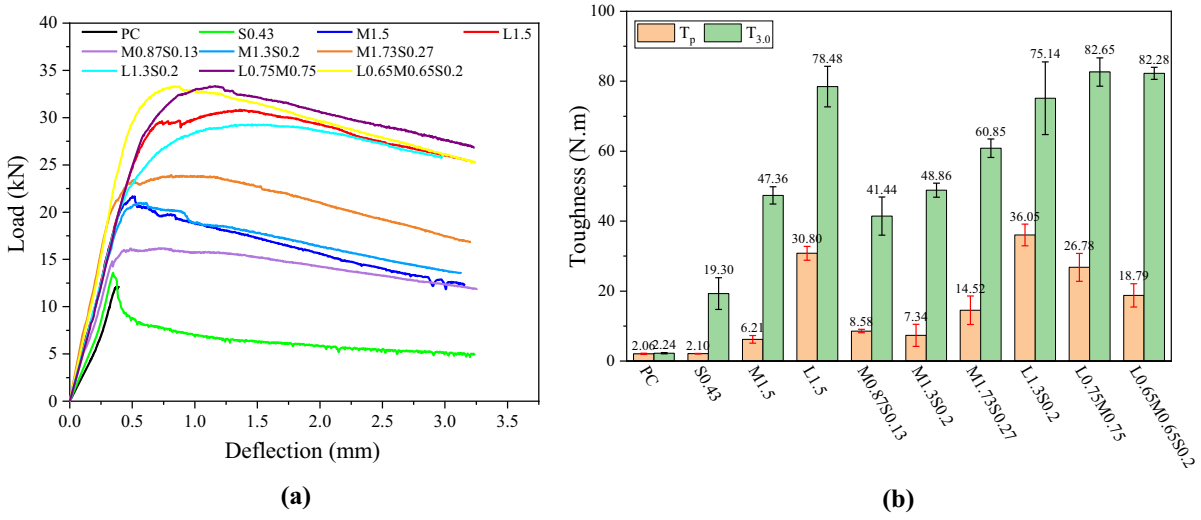

Fig. 12 Toughness of concrete mixtures: **a** typical Load–Deflection curves and **b** toughness T_p and $T_{3.0}$. Error bars show the standard deviation of 3 replicas

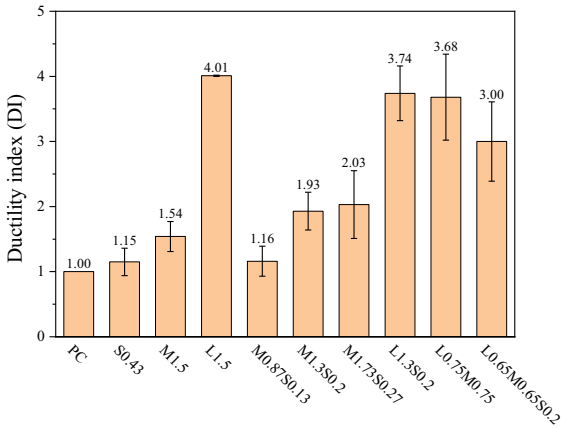

Fig. 13 Ductility index of concrete mixtures. Error bars show the standard deviation of 3 replicas

reinforced concrete increases with the volume fraction of hybrid fiber. T_p and $T_{3.0}$ increase from 8.58 to 14.52 N m and 41.44 to 60.85 N m. The hybrid fibers with different combination types produce other effects on toughness. The synergistic effect on toughness is observed in L0.65M0.65S0.2 and L0.75M0.75, as the T_p and $T_{3.0}$ are higher than L1.5. But L1.3S0.2 has a lower $T_{3.0}$ than that of L1.5, which shows the marginal effect of the short fibers.

Overall, fiber reinforced concrete had a deflection hardening behavior before the peak load (see Fig. 9a and Fig. 12a), with enhanced global bending deformation [38]. In this study, LOP is considered as the load for the onset of the first crack. For concrete mixtures, except for PC, the peak load is higher than LOP, which highlights the ductility of the materials. Here, the ductility index (DI) is adopted to measure this property of the reinforced mixtures, defined by the following relation [44]:

$$DI = \delta_P/\delta_{\mathrm{LOP}} \tag{3}$$

where δ_P is the deflection at the peak load and δ_{LOP} is the deflection at LOP. The higher ductility index indicates the higher ductility before the peak load. The comparisons of DI are detailed in Fig. 13.

For the mono fibers, the long hooked-end steel fiber (L1.5) produced a noticeable improvement on the ductility index than other mono fibers. It is attributed to the higher bonding strength of long hooked-end steel fiber. The average ductility index increases from 1.16 to 1.93 when the volume fraction increases from 1.0% to 1.5%. But no further growth is observed when the volume fraction exceeds 1.5%. Compared with L1.5, hybrid fibers with different combination types (L0.65M0.65S0.2, L1.3S0.2, and L0.75M0.75) produce lower ductility as the average ductility index decreases from 4.01 to 3.00, 3.74, and 3.68. It is probably due to the short fibers' negligible effect in arresting the fracture's propagation after LOP as shown by the horizontal strain component ε_{xx} maps in Fig. 14.

The fracture pattern at peak load and post-peak 90% peak load is depicted in Fig. 14. The short wave-shaped steel fiber has a negligible effect on the fracture as the pattern is similar to that of PC. The hooked-end steel fibers created branched fracture as they bridged cracks and transfer stress across the cracks, leading to the improvement of the flexural performance. The fracture evolution changed from almost vertical shape to branching one when the volume fraction of hybrid fiber increased from 1.0 to 2.0%. The hybridization of long hooked-end steel fiber with other fibers widened the fracture process zone and increased the number of main cracks.

4 Hybridization effect evaluation

In this study, the hybridization effect of the steel fibers on flexural performance was quantitatively analyzed according to [45–47]. The hybridization effect coefficient (α) is defined as:

$$\alpha = \frac{f_{HC} - f_{PC}}{\sum_i (f_{Mi} - f_{PC})}\beta_i \tag{4}$$

where f_{HC} is the flexural strength of the hybrid fiber reinforced concrete, f_{PC} is the flexural strength of PC, f_{Mi} is the flexural strength of the mono fiber reinforced concrete (i = 1, 2, 3, where 1 = L1.5, 2 = M1.5, 3 = S0.43), $\beta_i = V_i/V_{Mi}$, where V_{Mi} is the volume fraction of the mono fiber reinforcement, and V_i is the volume fraction of fiber (i = 1, 2, 3, where 1 = L, 2 = M, 3 = S) in the considered hybrid mix. The hybrid fiber produces a positive effect on the flexural strength if $\alpha > 1$, it is regarded as negative hybrid effect if $\alpha < 1$. For the sake of comparison, the hybridization effect coefficient of the hybrid fiber mixes with total volume fraction of 1.5% is only presented.

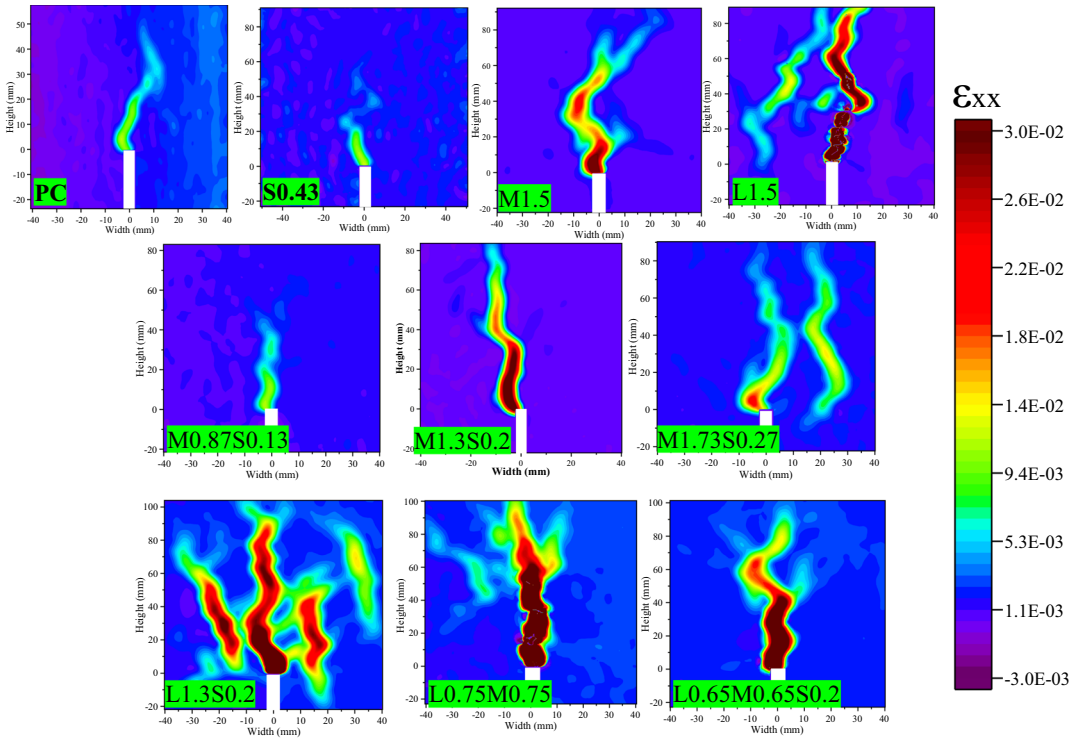
PC
S0.43
M1.5
L1.5
M0.87S0.13
M1.3S0.2
M1.73S0.27
L1.3S0.2
L0.75M0.75
L0.65M0.65S0.2
Height (mm)
Width (mm)
εxx
3.0E-02
2.6E-02
2.2E-02
1.8E-02
1.4E-02
9.4E-03
5.3E-03
1.1E-03
-3.0E-03

(a)

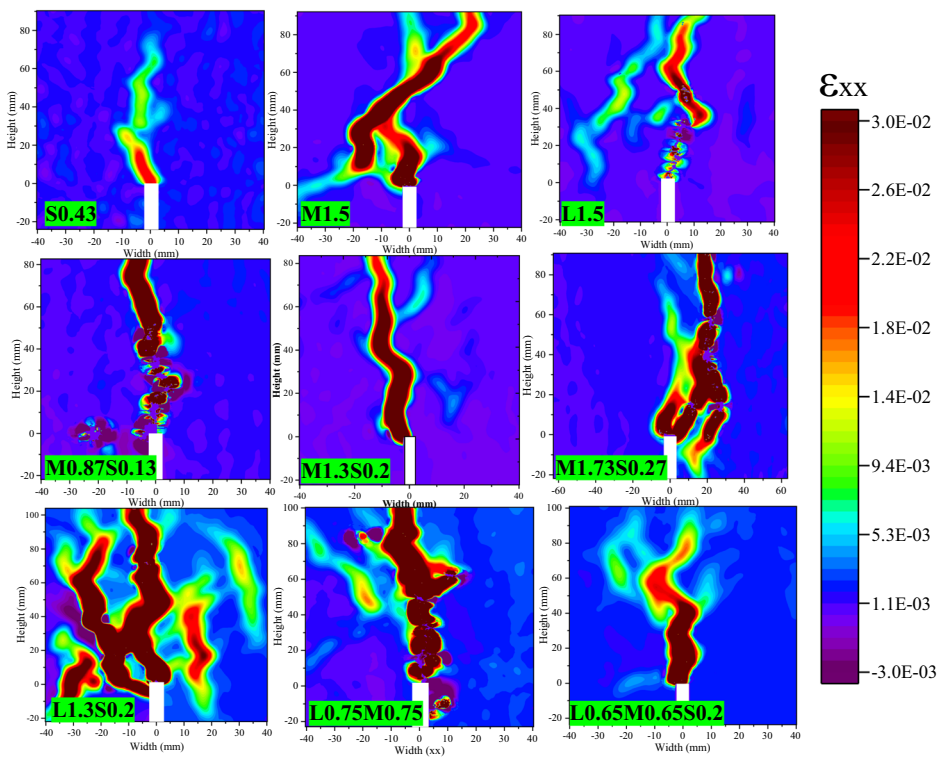
S0.43
M1.5
L1.5
M0.87S0.13
M1.3S0.2
M1.73S0.27
L1.3S0.2
L0.75M0.75
L0.65M0.65S0.2
Height (mm)
Width (mm)
Width (xx)
εxx
3.0E-02
2.6E-02
2.2E-02
1.8E-02
1.4E-02
9.4E-03
5.3E-03
1.1E-03
-3.0E-03

(b)

◀**Fig. 14** Map of horizontal strain component ε_{xx} at: **a** peak load, **b** post peak 90% peak load

The hybrid effect coefficient of the f_{LOP}, MOR, and $f_{2.5}$ are shown in Fig. 15. The hybrid fiber mix L0.65M0.65S0.2 and L0.75M0.75 produced a positive hybrid effect over the three parameters considered. The hybridization of steel fibers has negligible or negative effect when short fiber is mix with only L or M, except for L1.3S0.2 which had a positive hybrid effect on the first crack strength. Overall, the hybridization of the long and medium hooked-end steel fibers, which have the same aspect ratio but different lengths, produced a positive hybrid effect. A better effect was got when the mix contained the three steel fibers. A rough interpretation is: the hybridization of the long and medium hooked-end steel fiber can produce a better restriction effect on the initiation and propagation of the macro and meso cracks and better stress transfer [47], while the short wave-shaped steel fibers restrain the micro cracks. Therefore, the mix of the three fibers created the better hybridization effect with the highest values of α for L0.65M0.65S0.2.

5 Conclusions

The concrete reinforced with ten hybrid combinations of three different steel fiber shapes allowed to understand better the hybridization effect on the mixtures' mechanical performance. The main conclusions are:

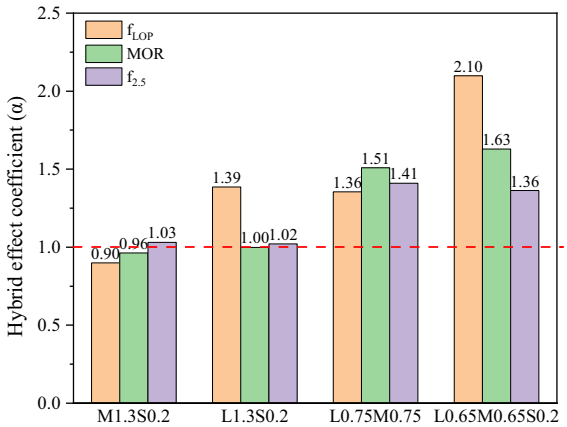

Fig. 15 Hybridization effect coefficient of hybrid fibers of the hybrid fiber mixes with total volume fraction of 1.5%

- The short wave-shaped steel fibers produced a more considerable reduction of workability than hooked-end steel fibers. The workability of the hybrid fiber reinforced concrete decreased with the volume fraction significantly particularly when the volume fraction exceeded 1.5%. The effect of the hybrid fiber including long hooked-end steel fiber on the workability varies with the hybridization type.
- Short wave-shaped steel fiber produced a lower autogenous shrinkage strain than hooked-end steel fibers. The long hooked-end steel fiber had a negligible effect on autogenous shrinkage. Shrinkage strain increased when the volume fraction of hybrid fiber (M + S) exceeds 1.0%. The hybrid reinforcement including long hooked-end steel fibers did not have synergistic effect on autogenous shrinkage.
- Mono steel fiber has no significant effect on compressive strength. The compressive strength decreases when the volume fraction increases from 1.0 to 1.5% but increases when it exceeds 1.5%. Hybrid fibers with different combination types produce a synergistic effect. A linear relationship was detected between shrinkage strain and compressive strength.
- Hooked-end steel fibers produced a more significant improvement of the tensile splitting strength than short wave-shaped steel fibers. An exponential relationship existed between tensile splitting strength and the volume fraction, for the considered concrete mixes, when the volume fraction increases from 0.0% to 2.0%. The ratio of tensile splitting strength to the compressive strength of hooked-end steel fiber reinforced concrete was estimated as 0.102.
- Concrete reinforced with steel fibers exhibited a pseudo strain hardening behavior. Steel fiber reinforcement improved flexural strength and fracture toughness. The long hooked-end steel fiber increased the MOR, residual strength, and toughness among the other fiber hybridizations. Flexural strength increased with the increasing volume fraction of the hybrid fibers. A linear relationship was detected between MOR and the volume fraction of hybrid fiber for the considered

concrete mixes. The ratio of MOR to compressive strength varied with different hybrid fibers. L0.65S0.65 and L0.75M0.75 produced a synergistic effect on MOR and toughness.
- The hybrid reinforced concrete L0.65M0.65S0.2 containing the three considered fiber types had the best performance according to the considered engineering properties and the hybridization effect coefficient.

The findings in this study can provide some contributions for the hybrid steel fiber reinforced concrete design according to the workability and mechanical properties needed in the construction applications. On the other hand, this study's relationship between mechanical properties provides necessary information for more accurate numerical modeling predictions, especially for the nonlinear simulation. Further investigations must be devoted to the durability and structural performance of the hybrid steel fiber reinforced concrete.

Acknowledgements The authors gratefully acknowledge TEKNA CHEM S.p.A. (Renate) and Mr. Silvio Cocco and Dr Valeria Campioni for the support to the research. Special thanks are due to Mr. Antonio Cocco and Mr. Daniele Spinelli (Materials Testing Laboratory, Politecnico di Milano) who supervised F. H. in setting up the experimental apparatus and performing the tests.

Author's contributions FH: Conceptualization, Methodology, Experiments, Data analysis, Writing. LB: Conceptualization, Methodology, Validation, Review and Editing. VC: Methodology, Data analysis, Validation, Review and Editing.

Funding Open access funding provided by Politecnico di Milano within the CRUI-CARE Agreement. No funding was received for conducting this study.

Declaration

Conflict of interest The authors have no competing interests to declare that are relevant to the content of this article.

References

1. Aitcin PC (2000) Cements of yesterday and today - Concrete of tomorrow. Cement Concrete Res 30(9):1349–1359. https://doi.org/10.1016/S0008-8846(00)00365-3
2. Turk K, Bassurucu M, Bitkin RE (2021) Workability, strength and flexural toughness properties of hybrid steel fiber reinforced SCC with high-volume fiber. Constr Build Mater. https://doi.org/10.1016/j.conbuildmat.2020.120944
3. Banthia N, Gupta R (2004) Hybrid fiber reinforced concrete (HyFRC): fiber synergy in high strength matrices. Mater Struct 37(10):707–716
4. Banthia N, Majdzadeh F, Wu J, Bindiganavile V (2014) Fiber synergy in hybrid fiber reinforced concrete (HyFRC) in flexure and direct shear. Cement Concrete Comp 48:91–97. https://doi.org/10.1016/j.cemconcomp.2013.10.018
5. Xie ZL, Zhou HF, Lu LJ, Chen ZA (2017) An investigation into fracture behavior of geopolymer concrete with digital image correlation technique. Constr Build Mater 155:371–380. https://doi.org/10.1016/j.conbuildmat.2017.08.041
6. Bencardino F, Rizzuti L, Spadea G, Swamy RN (2010) Experimental evaluation of fiber reinforced concrete fracture properties. Compos Part B-Eng 41(1):17–24. https://doi.org/10.1016/j.compositesb.2009.09.002
7. Choi Y, Yuan RL (2005) Experimental relationship between splitting tensile strength and compressive strength of GFRC and PFRC. Cement Concrete Res 35(8):1587–1591. https://doi.org/10.1016/j.cemconres.2004.09.010
8. Qian C, Stroeven P (2000) Fracture properties of concrete reinforced with steel–polypropylene hybrid fibres. Cement Concr Compos 22(5):343–351. https://doi.org/10.1016/S0958-9465(00)00033-0
9. Li VC, Stang H, Krenchel H (1993) Micromechanics of crack bridging in fibre-reinforced concrete. Mater Struct 26(8):486–494. https://doi.org/10.1007/BF02472808
10. Yoo D, Lee J, Yoon Y (2013) Effect of fiber content on mechanical and fracture properties of ultra high performance fiber reinforced cementitious composites. Compos Struct 106:742–753. https://doi.org/10.1016/j.compstruct.2013.07.033
11. Liu X, Sun Q, Yuan Y, Taerwe L (2020) Comparison of the structural behavior of reinforced concrete tunnel segments with steel fiber and synthetic fiber addition. Tunn Undergr Sp Tech 103:103506. https://doi.org/10.1016/j.tust.2020.103506
12. Wang ZL, Zhu HH, Wang J, Zhu B (2012) Experimental study on macroscopic mechanical behavior of SFRC under triaxial compression. Mech Adv Mater Struc 19(8):653–662
13. Ren GM, Wu H, Fang Q, Liu JZ (2018) Effects of steel fiber content and type on static mechanical properties of UHPCC.

Constr Build Mater 163:826–839. https://doi.org/10.1016/j.conbuildmat.2017.12.184
14. Wu Z, Shi C, Khayat KH (2019) Investigation of mechanical properties and shrinkage of ultra-high performance concrete: Influence of steel fiber content and shape. Compos B Eng 174:107021. https://doi.org/10.1016/j.compositesb.2019.107021
15. Mehta P, Monteiro P (2014) Concrete: microstructure, properties, and materials. McGraw-Hill Education, New York
16. Soroushian P, Elyamany H, Tlili A, Ostowari K (1998) Mixed-mode fracture properties of concrete reinforced with low volume fractions of steel and polypropylene fibers. Cement Concr Compos 20(1):67–78. https://doi.org/10.1016/S0958-9465(97)87390-8
17. Sun L, Hao Q, Zhao J, Wu D, Yang F (2018) Stress strain behavior of hybrid steel-PVA fiber reinforced cementitious composites under uniaxial compression. Constr Build Mater 188:349–360. https://doi.org/10.1016/j.conbuildmat.2018.08.128
18. Lawler JS, Wilhelm T, Zampini D, Shah SP (2003) Fracture processes of hybrid fiber-reinforced mortar. Mater Struct 36(3):197–208
19. Lee J, Cho B, Choi E, Kim Y (2016) Experimental study of the reinforcement effect of macro-type high strength polypropylene on the flexural capacity of concrete. Constr Build Mater 126:967–975. https://doi.org/10.1016/j.conbuildmat.2016.09.017
20. Cao Q, Cheng Y, Cao M, Gao Q (2017) Workability, strength and shrinkage of fiber reinforced expansive self-consolidating concrete. Constr Build Mater 131:178–185. https://doi.org/10.1016/j.conbuildmat.2016.11.076
21. Yakhlaf M, Safiuddin M, Soudki KA (2013) Properties of freshly mixed carbon fibre reinforced self-consolidating concrete. Constr Build Mater 46:224–231. https://doi.org/10.1016/j.conbuildmat.2013.04.017
22. Gopalaratnam VS, Gettu R (1995) On the characterization of flexural toughness in fiber reinforced concretes. Cement Concr Compos 17(3):239–254. https://doi.org/10.1016/0958-9465(95)99506-O
23. Liu F, Ding W, Qiao Y (2019) Experimental investigation on the flexural behavior of hybrid steel-PVA fiber reinforced concrete containing fly ash and slag powder. Constr Build Mater 228:116706. https://doi.org/10.1016/j.conbuildmat.2019.116706
24. Nunes LCS, Reis JML (2012) Estimation of crack-tip-opening displacement and crack extension of glass fiber reinforced polymer mortars using digital image correlation method. Mater Des 33:248–253. https://doi.org/10.1016/j.matdes.2011.07.051
25. A. Proof, TEKNA CHEM S.p.A. https://www.teknachemgroup.com/public/allegato/st_aeternum_proof_v2020rev1_en.pdf).
26. EN 206:2013+A1:2016, Concrete - Specification, performance, production and conformity.
27. EN 12390–2:2019, Testing hardened concrete, Part 2: Making and curing specimens for strength test.
28. EN 12390–3:2019, Testing hardened concrete, Part 3: Compressive strength of test specimens.
29. EN 12390–6:2009, Testing hardened concrete, Part 6: Tensile splitting strength of test specimens.
30. EN 14651:2005+A1:2007, Test method for metallic fiber concrete. Measuring the flexural tensile strength (limit of proportionality (LOP), residual).
31. EN 12390–16:2019, Testing hardened concrete, Part 16: Determination of the shrinkage of concrete.
32. EN 2350–2:2019, Testing fresh concrete, Part 2: Slump test.
33. Liu X, Wu T, Yang X, Wei H (2019) Properties of self-compacting lightweight concrete reinforced with steel and polypropylene fibers. Constr Build Mater 226:388–398. https://doi.org/10.1016/j.conbuildmat.2019.07.306
34. Rasoolinejad M, Rahimi-Aghdam S, Bažant ZP (2019) Prediction of autogenous shrinkage in concrete from material composition or strength calibrated by a large database, as update to model B4. Mater Struct 52(2):33. https://doi.org/10.1617/s11527-019-1331-3
35. Tazawa E, Miyazawa S, Kasai T (1995) Chemical shrinkage and autogenous shrinkage of hydrating cement paste. Cement Concrete Res 25(2):288–292. https://doi.org/10.1016/0008-8846(95)00011-9
36. Sun W, Chen H, Luo X, Qian H (2001) The effect of hybrid fibers and expansive agent on the shrinkage and permeability of high-performance concrete. Cement Concrete Res 31(4):595–601. https://doi.org/10.1016/S0008-8846(00)00479-8
37. Mazzoli A, Monosi S, Plescia ES (2015) Evaluation of the early-age-shrinkage of Fiber Reinforced Concrete (FRC) using image analysis methods. Constr Build Mater 101:596–601. https://doi.org/10.1016/j.conbuildmat.2015.10.090
38. Akça KR, Çakır Ö, İpek M (2015) Properties of polypropylene fiber reinforced concrete using recycled aggregates. Constr Build Mater 98:620–630. https://doi.org/10.1016/j.conbuildmat.2015.08.133
39. Lin SHAC, Stress-strain behavior of steel-fiber high-strength concrete under compression, ACI Struct J, https://doi.org/10.14359/4152.
40. Itim A, Ezziane K, Kadri E (2011) Compressive strength and shrinkage of mortar containing various amounts of mineral additions. Constr Build Mater 25(8):3603–3609. https://doi.org/10.1016/j.conbuildmat.2011.03.055
41. Tang S, Huang D, He Z (2021) A review of autogenous shrinkage models of concrete. J Build Eng 44:103412. https://doi.org/10.1016/j.jobe.2021.103412
42. Nataraja MC, Dhang N, Gupta AP (2001) Splitting tensile strength of SFRC. Indian Concr J. 75(4):287–289
43. Singh H (2017) Steel fiber reinforced concrete: behavior, modelling and design, Springer Transactions in Civil and Environmental Engineering,SPRINGER-VERLAG SINGAPORE PTE LTD, SINGAPORE, pp. 1–172
44. Shaikh FUA (2013) Deflection hardening behaviour of short fibre reinforced fly ash based geopolymer composites. Mater Des 50:674–682. https://doi.org/10.1016/j.matdes.2013.03.063
45. Song W, Yin J (2016) Hybrid effect evaluation of steel fiber and carbon fiber on the performance of the fiber reinforced concrete. Materials 9(8):704. https://doi.org/10.3390/ma9080704
46. Feng J, Gao X, Li J, Dong H, Yao W, Wang X, Sun W (2019) Influence of fiber mixture on impact response of ultra-high-performance hybrid fiber reinforced cementitious

composite. Compos B Eng 163:487–496. https://doi.org/10.1016/j.compositesb.2018.12.141
47. Xu L, Huang L, Chi Y, Mei G (2016) Tensile behavior of steel-polypropylene hybrid fiber-reinforced concrete. ACI Mater J 113(2):219–229